JOURNAL OF SOLID STATE CHEMISTRY 85, 332–336 (1990)

The Structure of α-$Mo_{15}Se_{19}$, a Binary Molybdenum Selenide Containing Mo_6Se_8 and Mo_9Se_{11} Clusters

BARRY D. DAVIS AND WILLIAM R. ROBINSON*

Department of Chemistry, Purdue University, West Lafayette, Indiana 47907-3699

Received August 28, 1989; in revised form December 1, 1989

Single crystals of α-$Mo_{15}Se_{19}$ (hexagonal, space group $P6_3/m$, $a = 9.450(2)$, $c = 19.600(2)$ Å) were prepared by deintercalation of $In_3Mo_{15}Se_{19}$ with iodine. The structure was determined from an X-ray data set of 726 unique reflections ($R = 0.050$, $R_w = 0.070$). The dimensions of the Mo_6Se_8 cluster in this compound are not significantly different from those in β-$Mo_{15}Se_{19}$. The mean metal–metal distance in the Mo_9Se_{11} cluster is identical to that in the β phase, although individual distances differ significantly. This may be attributable to the differences in packing between the two isoelectronic phases.

Introduction

Metal–metal bonding in low valent molybdenum complexes produces molybdenum chalcogenides containing Mo_6 octahedra (*1, 2*) or more extended clusters resulting from the confacial condensation of Mo_6 octahedra (*3–7*). Crystals of these clusters contain channels, or gaps between clusters, which may be intercalated by various metal atoms. Yvon (*2*) established distinct trends in Mo–Mo bond shrinkage upon increased formal charge of the intercalated metal atom for the $M_xMo_6Se_8$ series. Thus, the intercalated metal atom may be viewed as donating electrons into bonding orbitals of the clusters. The trends in Mo–Mo bond lengths are also observed for Mo_9Se_{11} clusters. For example, β-$M_xMo_{15}Se_{19}$ systems, which are composed of two distinct molybdenum clusters, Mo_6Se_8 and Mo_9Se_{11} (*15*), exhibit modest contractions of the Mo–Mo bonds upon indium intercalation. However, the behavior of the α-$M_xMo_{15}Se_{19}$ systems (*8*) is inconsistent with the observed trends in the β series. Although β-$M_xMo_{15}Se_{19}$ and binary β-$Mo_{15}Se_{19}$ systems have been studied and the Mo–Mo bond lengths compared (*14–17*), no studies of the binary α-$Mo_{15}Se_{19}$ phase have been reported. We present the preparation and characterization of single crystals of the α form of $Mo_{15}Se_{19}$ and report the comparison of its Mo–Mo bond lengths to those of α-$M_xMo_{15}Se_{19}$ and the β phases.

* Author to whom correspondence should be addressed.

0022-4596/90 $3.00

Experimental

Black, shiny needles of α-$Mo_{15}Se_{19}$ were isolated as a minor phase from a deintercalation reaction of $In_2Mo_6Se_6$ (*6, 7*) and I_2. The charge was placed in an evacuated glass tube with a stoichiometric amount of I_2 and heated in a temperature gradient from 400°C to room temperature. Deintercalation of indium atoms from $In_{\sim3}Mo_{15}Se_{19}$ crystals, a possible contaminant at the cool end of the tube, produced needles of α-$Mo_{15}Se_{19}$.

The black needle used for data collection was mounted on a glass fiber with its long axis roughly parallel to the ϕ axis of the goniometer. Data collection and refinement parameters are outlined in Table I. The structure was solved using a combination of Patterson and difference Fourier methods and was refined by full-matrix least-squares techniques.

The 379 reflections having intensities greater than 3.0 times their standard deviation were used in the refinements. The final cycle of refinement included 55 variable parameters and converged with unweighted and weighted agreement factors: $R = 0.050$ and $R_{wt} = 0.070$. The crystal appeared to be effectively free of indium. Attempts at refining 5% occupancy levels at the possible indium sites led to very large temperature factors. Also, no electron density was observed at these sites in the Fourier differ-

TABLE I

Crystal Data and Data Collection Parameters

Formula	$Mo_{15}Se_{19}$
Formula weight	2939.34
Space group	$P6_3/m$ (No. 176)
a (Å)	9.450(2)
c (Å)	19.600(2)
V (Å^3)	1515.8(8)
Z	2
d_{calc} (g cm^{-3})	6.439
Crystal dimensions (mm)	0.05 × 0.05 × 0.12
Temperature (°C)	23.
Radiation (wavelength)	Mo$K\alpha$ (0.71073 Å)
Monochromator	Graphite
Linear abs. coef. (cm^{-1})	284.32
Absorption correction applied	Empirical[a]
Transmission factors: min, max	0.66, 1.00
Diffractometer	Enraf-Nonius CAD4
Scan method	ω-2θ
h, k, l limits:	−10 to 8, 0 to 10, 0 to 21
2θ range (deg)	6.00–46.00
Scan width (deg)	1.00 + 0.35 tan(θ)
Take-off angle (deg)	2.80
Programs used	Enraf-Nonius SDP
F_{000}	2552.0
p-Factor used in weighting	0.040
Data collected	1634
Unique data	726
Agreement factor (on I)	0.048
Data with $I > 3.0\sigma(I)$	379
Number of variables	55
Largest shift/esd in final cycle	0.03
R	0.050
R_w	0.070
Goodness of fit	1.766

[a] N. Walker and D. Stuart, *Acta Crystallogr. Sect. A* **39,** 158 (1983).

TABLE II

Table of Positional Parameters and Their Estimated Standard Deviations

Atom	x	y	z	B (A^2)
(Se1)	0	0	0.1618(3)	0.94(9)
(Se2)	0.33333	0.66666	0.5314(3)	1.25(9)
(Se3)	0.3021(5)	0.3379(6)	0.75	0.9(1)
(Se4)	0.0378(4)	0.3300(4)	0.0473(1)	0.71(7)
(Se5)	−0.0013(4)	0.3744(4)	0.6441(2)	0.69(7)
(Mo1)	0.4889(5)	0.6504(5)	0.75	0.85(9)
(Mo2)	0.1731(3)	0.1526(3)	0.0607(1)	0.66(6)
(Mo3)	0.1813(3)	0.6885(4)	0.6327(1)	0.84(6)

Note. Anisotropically refined atoms are given in the form of the isotropic equivalent thermal parameter defined as:

$$(\tfrac{4}{3}) * [a^2 * \beta(1,1) + b^2 * \beta(2,2) + c^2 * \beta(3,3) + ab(\cos\gamma) * \beta(1,2) + ac(\cos\beta) * \beta(1,3) + bc(\cos\alpha) * \beta(2,3)].$$

TABLE III

Bond	α-$Mo_{15}Se_{19}$	β-$Mo_{15}Se_{19}$[a]	$In_{3.3}Mo_{15}Se_{19}$[b]	Sym. code
		Intracluster distances of Mo_9Se_{11} unit		
Mo(1)–Mo(1)	2.688(7)	2.697	2.768(10)	a
Mo(1)–Mo(3)	2.752(4)	2.719	2.757(7)	b
–Mo(3)	2.796(4)	2.830	2.771(7)	a
Mo(1)–Se(3)	2.573(7)		2.584(14)	a
–Se(3)	2.574(6)		2.609(14)	
Mo(1)–Se(5)	2.522(4)		2.596(5)	a
Mo(3)–Mo(3)	2.685(5)	2.677	2.655(7)	a
Mo(3)–Se(2)	2.519(6)		2.517(7)	
Mo(3)–Se(3)	2.703(4)		2.692(5)	b
Mo(3)–Se(5)	2.591(4)		2.568(10)	
–Se(5)	2.595(4)		2.635(10)	b
Se(2) –Se(5)	3.711(5)		3.649(7)	
Se(3) –Se(5)	3.565(5)		3.583(10)	a
–Se(5)	3.693(6)		3.834(7)	
		Intracluster distances of Mo_6Se_8 unit		
Mo(2)–Mo(2)	2.837(4)	2.827	2.693(7)	−c
–Mo(2)	2.682(4)	2.675	2.688(7)	c
Mo(2)–Se(1)	2.515(5)		2.547(9)	
Mo(2)–Se(4)	2.541(4)		2.557(6)	−c
–Se(4)	2.568(5)		2.573(11)	d
–Se(4)	2.581(6)		2.628(11)	
Se(1) –Se(1)	3.459(8)		3.473(14)	−e
Se(1) –Se(4)	3.711(5)		3.663(8)	
Se(4) –Se(4)	3.489(5)		3.620(6)	−c
		Intercluster distances		
Mo(2)–Mo(3)	3.221(5)		3.512(8)	f
Mo(2)–Se(5)	2.593(4)		2.661(6)	g
Mo(3)–Se(4)	2.599(5)		2.665(6)	h
Se(1) –Se(1)	3.459(8)		3.473(14)	−i
Se(1) –Se(3)	3.496(4)		3.745(10)	g
Se(1) –Se(5)	3.561(4)		3.720(7)	g
Se(2) –Se(4)	3.379(4)		3.577(8)	−e
–Se(4)	3.537(4)		3.649(7)	j
Se(4) –Se(5)	3.534(5)		3.582(9)	k
–Se(5)	3.540(5)		3.601(6)	g
–Se(5)	3.812(4)		3.754(6)	−e

Note. (a) $1 - y, x - y + 1, z$; (b) $y - x, 1 - x, z$; (c) $-y, x - y, z$; (d) $y - x, -x, z$; (e) $-x, -y, 0.5 + z$; (f) $x - y + 1, x, 1.5 + z$; (g) $y, y - x, -0.5 + z$; (h) $-x, 1 - y, 0.5 + z$; (i) $y, y - x, 0.5 + z$; (j) $x - y, x, -0.5 + z$; (k) $-x, 1 - y, -0.5 + z$. Negative sign before the letter implies the inversion operation.

[a] Ref. (*9*). Neither atomic positions nor standard deviations were reported.

[b] Ref. (*8*).

ence map. Final atomic positions are reported in Table II and bond distances in Table III. A table of observed and calculated structure factures and a table of anisotropic temperature factors are available from one of the authors (W.R.R.)

Discussion

Like other $Mo_{15}Se_{19}$ derivatives, crystalline α-$Mo_{15}Se_{19}$ is composed of two molybdenum selenide clusters: Mo_6Se_8 and Mo_9Se_{11} (Fig. 1). The Mo_6Se_8 unit consists of an octahedron of molybdenum atoms with selenium atoms bridging each triangular face. The selenium atoms lie at the vertices of a cube with Mo atoms in each face. The Mo_6Se_8 cluster in α-$Mo_{15}Se_{19}$ has the same dimensions as the cluster in Mo_6Se_8 (*13*) and in β-$Mo_{15}Se_{19}$ (*9*). The Mo_9Se_{11} unit may be thought of as two Mo_6Se_8 units which have been fused along one face of the Mo_6 octahedron forming a confacial bioctahedron of molybdenum. The selenium atoms bridge each triangular face. The three selenium atoms which are coplanar with the shared octahedral face bridge two triangular faces—one on each octahedron. The dimensions within the Mo_9Se_{11} clusters differ slightly in α- and β-$Mo_{15}Se_{19}$.

Binary $Mo_{15}Se_{19}$ exists in two crystallographic forms, a hexagonal α phase and a rhombohedral β phase. These differences, which also may be seen in the parent ternary systems, have been described by Chevrel, *et al.* (*9*) and by Tarascon and Murphy (*16*) in terms of the sequences of clusters in the *c*-direction about centers at (0, 0, *z*) and ($\frac{2}{3}$, $\frac{1}{3}$, *z*). The α phase consists of two different sequences: a series of Mo_6Se_8–Mo_6Se_8–Mo_6Se_8 clusters along the threefold axes at (0, 0, *z*) and a series of Mo_9Se_{11}–Mo_9Se_{11}–Mo_9Se_{11} clusters along the threefold axes at ($\frac{2}{3}$, $\frac{1}{3}$, *z*). The β phase consists of a single sequence of Mo_6Se_8–Mo_9Se_{11}–Mo_6Se_8 clusters along each threefold axis. The α phase has C_{3h} symmetry about the Mo_9Se_{11} cluster, while the β phase has D_3 symmetry about the Mo_9Se_{11} cluster.

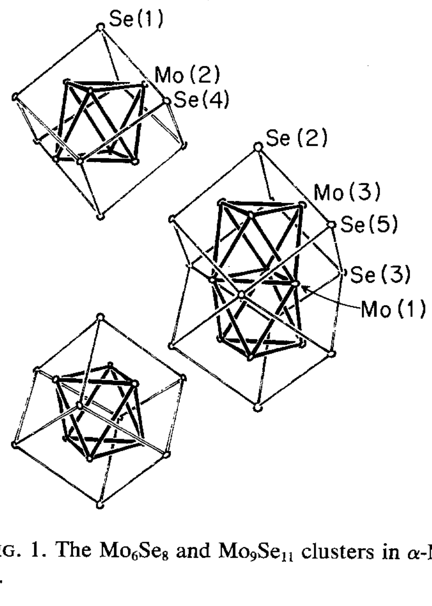

FIG. 1. The Mo_6Se_8 and Mo_9Se_{11} clusters in α-$Mo_{15}Se_{19}$.

For the Mo_6 cluster, the differences in Mo–Mo bond lengths between α-$Mo_{15}Se_{19}$ (*8*) and $In_{\sim 3}Mo_{15}Se_{19}$ are consistent with indium donating electrons to the molybdenum clusters (*10*). Like the β phase, the Mo_6Se_8 cluster of the α phase becomes more symmetrical via contraction upon increasing ternary intercalation (Table III). However, the Mo–Mo bond lengths in the Mo_9 cluster of the α phase of $In_{\sim 3}Mo_{15}Se_{19}$ differ slightly from those in the β phase, and these differences become more pronounced at high ternary concentration. In the indium intercalated α systems, the Mo_9Se_{11} cluster is more uniform than that in the binary phase. Intercalation produces a mild contraction of the Mo–Mo bonds both along the threefold axis and in the median triangle [Mo(1)–Mo(1)], along with an elongation in the outer triangles [Mo(3)–Mo(3)]. These changes differ from the β phase, which contracts along the threefold axis and elongates at the median. The differences in behavior of the Mo(1)–Mo(3) bonds upon intercalation are indicative of a twisting of the molybdenum triangles about the threefold axis. However, the twisting does not cause any differences between interplanar spacings [between the Mo(1) triangles and the Mo(3) triangles]. The intercluster selenium–selenium distances, molybdenum–molybdenum bonds, and molybdenum–selenium bonds between the Mo_6Se_8 and Mo_9Se_{11} units of α-$Mo_{15}Se_{19}$ lengthen with increasing indium concentration. Thus for the binary α-$Mo_{15}Se_{19}$, the intercluster distances are shortened to distances which are comparable to intracluster bond lengths.

In summary, addition of indium to α-$Mo_{15}Se_{19}$ results in changes in the Mo–Mo bond lengths of the Mo_6 cluster which are similar to those in the β system. Also, indium addition results in changes of the Mo–Mo bond lengths in the Mo_9 cluster of the α phase which are different from those in the β phase. From changes in the Mo(1)–Mo(3) bond lengths, rotation about the threefold axis may be inferred to be among the differences between the α and β phases.

Acknowledgment

We thank Dr. Phillip Fanwick for his assistance in solving the crystal structure.

References

1. O. Fischer, *Appl. Phys.* **16**, 1 (1978).
2. K. Yvon, "Current Topics in Material Science," Vol. III. North-Holland, Amsterdam (1978).
3. R. Chevrel, M. Potel, M. Sergent, M. Decroux, and O. Fischer, *J. Solid State Chem.* **34**, 247 (1980).
4. P. Gougeon, M. Potel, J. Papdiou, and M. Sergent, *Mater. Res. Bull.* **22**, 1087 (1987).
5. P. Gougeon, M. Potel, J. Papdiou, and M. Sergent, *Mater. Res. Bull.* **23**, 453 (1988).
6. W. Honle, H. G. Von Schnering, A. Lipka, and K. Yvon, *J. Less-Common Metals* **71**, 135 (1980).
7. M. Potel, R. Chevrel, M. Sergent, J. C. Armici, M. Decroux, and O. Fischer, *J. Solid State Chem.* **35**, 286 (1980).
8. A. Gruttner, K. Yvon, R. Chevrel, M. Potel, M. Sergent, and B. Seeber, *Acta. Crystallogr. Sect. B* **35**, 285 (1979).
9. M. Potel, P. Grougeon, R. Chevrel, and M. Sergent, *Rev. Chim. Miner.* **21**, 509 (1984).
10. J. M. Tarascon, G. W. Hull, and J. V. Waszczak, *Mater. Res. Bull.* **20**, 935 (1985).
11. R. Chevrel, M. Sergent, B. Seeber, O. Fischer, A. Gruttner, and K. Yvon, *Mater. Res. Bull.* **14**, 567 (1979).
12. J.M. Tarascon, F. J. DiSalvo, D. W. Murphy, G. Hull, and J. V. Waszczak, *Phys. Rev. B* **29**(1), 172 (1984).
13. O. Bars, J. Guillevic, and D. Grandjean, *J. Solid State Chem.* **6**, 48 (1973).
14. J. M. Tarascon and G. W. Hull, *Mater. Res. Bull.* **21**, 859 (1986).
15. R. Chevrel, M. Potel, M. Sergent, M. Decroux, and O. Fischer, *Mater. Res. Bull.* **15**, 867 (1980).
16. J. M. Tarascon and D. W. Murphy, *Phys. Rev. B* **33**(4), 2625 (1986).
17. J. M. Tarascon, *Solid State Ionics* **18**, 768 (1986).